**The Stretching of a Slender, Axisymmetric, Viscous Inclusion--Part II: Numerical Solution and Results**

A. D. Fitt; P. Wilmott

*SIAM Journal on Applied Mathematics*, Vol. 49, No. 6. (Dec., 1989), pp. 1617-1634.

Stable URL:
http://links.jstor.org/sici?sici=0036-1399%28198912%2949%3A6%3C1617%3ATSOASA%3E2.0.CO%3B2-U

*SIAM Journal on Applied Mathematics* is currently published by Society for Industrial and Applied Mathematics.

---

SIAM J. APPL. MATH.
Vol. 49, No. 6, pp. 1617-1634, December 1989

004

# THE STRETCHING OF A SLENDER, AXISYMMETRIC, VISCOUS INCLUSION–PART II: NUMERICAL SOLUTION AND RESULTS*

A. D. FITT† AND P. WILMOTT‡

**Abstract.** In Part I [*SIAM J. Appl. Math.*, 49 (1989), pp. 1608-1616] of this paper, the stretching of a thin, axisymmetric, viscous inclusion was examined via the method of matched asymptotic expansions, resulting in a coupled system consisting of a nonlinear integrodifferential equation and a first-order conservation law. Now the numerical solution of this problem is considered, that relies on the approximation of the unknown functions in the integrodifferential equation in terms of the products of cubic splines coupled to a timestepping solution of the conservation law. Some results are given and comparisons made with the known exact solutions. Consideration is also given to cases where no exact solution is available.

**Key words.** integrodifferential equations, slow viscous flow, numerical solution of equations

**AMS(MOS) subject classifications.** 45K05, 65N05, 65R20, 76D99

**1. Introduction.** In Part I of this paper [7] the analysis of the stretching of a thin, axisymmetric, viscous inclusion was examined. Part II of the paper considers the numerical solution of the resulting coupled system of a nonlinear integrodifferential equation and a first-order conservation law, giving a selection of results. There is not an extensive literature on the type of integrodifferential equation that arises in the problem. Spence and Sharp [6] used Chebyshev polynomials to solve a similar equation resulting from the study of an elastohydrodynamic cavity flow in two dimensions, but the nature of the kernel of the present equation makes this choice of basis functions inappropriate. We have chosen to employ cubic splines for reasons that will become apparent below, and some attention has been given to methods such as this in [2]. In [1] Baker considers some closely related integral equations but gives no methods that are directly applicable to our case. The numerical solution of a number of different types of singular nonlinear integrodifferential equations has been discussed previously in [4] and [5] for problems arising from the study of separated flow. Although in some ways the equations bear a superficial resemblance to the present problem and the basic numerical strategy is the same, the problems are totally different in practice.

The interested reader is referred to Part I [7] for a full description of the problem. Briefly, we assume that a highly viscous fluid of viscosity $\mu$ contains a slender, axisymmetric inclusion of viscosity $\eta$. Defining the viscosity ratio as $\delta = \mu/\eta$ and the initial halflength of the inclusion as $L$, we assume that the unperturbed external flow is of pure shear (stagnation point) type and has velocity components

$$u = \gamma x, \qquad v = -\frac{\gamma r}{2}$$

where the $x$-axis is aligned with the axis of the inclusion. If we define the slenderness parameter $\varepsilon$ in terms of the volume $V$ of the inclusion (that of course remains constant throughout the flow due to the incompressibility of the viscous fluid) by

$$V = \frac{4\pi\varepsilon^2 L^3}{3},$$

* Received by the editors September 28, 1988; accepted for publication November 28, 1988.

† Mathematics Group, Royal Military College of Science, Shrivenham, Swindon, Wiltshire, United Kingdom.

‡ Department of Mathematics, Imperial College, London, United Kingdom.

then it is possible to show that for a fixed ratio $\delta$ the regime of interest where the two fluids interact with each other corresponds to $\delta = O(\varepsilon^2)$. To make this precise, we define the parameter $\lambda$, of order unity, by

$$\delta = \lambda \varepsilon^2$$

and the flow problem may then be solved using the method of matched asymptotic expansions (Part I, [7]).

It is worth mentioning at this point that some of the numerical interest in the problem stems from the fact that the relevant integral, while not of singular type, is coupled to an essentially nonlinear conservation law evolution equation and so some care is needed in combining the timestepping procedure for the differential equation and the solution procedure for the integral equation.

**2. Equations of motion.** The method of matched asymptotic expansions applied to the problem as described in Part I leaves us with the following partial differential and integrodifferential equations to solve

$$A_t + (Au)_x = 0, \tag{1}$$

$$x + 2\int_{-l_1(t)}^{l_2(t)} \frac{\beta(s,t)-\beta(x,t)}{|s-x|}\,ds + 2\beta(x,t)(-1+\log[4(l_2-x)(l_1+x)]) = u + 2\beta(x,t)\log\left(\frac{A\varepsilon^2}{\pi}\right) \tag{2}$$

where $A(x, t)$ is the cross-sectional area of the viscous inclusion (that has been scaled with $\varepsilon^2$), $-l_1(t)$ and $l_2(t)$ are the positions of the inclusion ends, $u(x, t)$ is the velocity of the inclusion, $\varepsilon$ has already been defined in the previous section, and

$$\beta = \frac{3}{8\pi\lambda}(Au_x)_x.$$

For simplicity, assume that the inclusion is symmetrical, so that $l_1(t) = l_2(t) = l(t)$ and the halflength $l(0)$ initially is unity. The assumption of symmetry is made at this stage only on the grounds of convenience: all of the coefficients that will be set up for the numerical solution of the problem will be for the more general asymmetrical case.

Under these assumptions (2) is modified to read

$$2\int_{-l(t)}^{l(t)} \frac{\beta(s,t)-\beta(x,t)}{|s-x|}\,ds + 2\beta(x,t)\left(-1-\log\left(\frac{\varepsilon^2}{4\pi}\right)+\log\left[\frac{l^2-x^2}{A}\right]\right) + x - u = 0. \tag{3}$$

The boundary conditions are that the cross-sectional area of the inclusion must be zero at the inclusion tips and that the velocities at the tips of the inclusions must be equal to the time derivatives of the inclusion length so that

$$A = 0 \quad \text{at } x = \pm l(t), \tag{4}$$

$$u = \pm \dot{l} \quad \text{at } x = \pm l(t). \tag{5}$$

There exist exact solutions to (1) and (2). These are given in full in Part I [7].

**3. Numerical solution procedure.** Before embarking on the numerical solution of the problem, it is convenient to make the following transformations to the equations of motion. We rescale the interval to fix the finite-difference mesh by setting

$$x = l(t)z, \qquad A(x,t) = l^2(t)a(z,t)$$

and also put

$$B=\frac{8\pi\lambda}{3}\beta, \quad s=l(t)p \quad \text{in the integral.}$$

We then have

$$\int_{-1}^{1}\frac{B(p,t)-B(z,t)}{|p-z|}\,dp+B(z,t)\left[C+\log\left(\frac{1-z^2}{a}\right)\right]+\frac{4\pi\lambda}{3}(lz-u)=0, \tag{6}$$

$$(l^3a)_t+[l^2ua-z\dot{l}l^2a]_z=0,$$

$$B=[au_z]_z, \tag{7}$$

$$a(\pm1)=0, \qquad u(\pm1)=\pm\dot{l}(t)$$

where

$$l(0)=1, \qquad C=-1-\log\left(\frac{\varepsilon^2}{4\pi}\right).$$

In brief, the numerical strategy will be as follows. The integrodifferential equation will be solved at time $t$ by collocation to provide an updated approximation for $u$, assuming a "known" scaled cross-sectional area $a(x, t)$. The new positions of the ends of the inclusion may then be calculated via the formula

$$l(t+dt)=l(t)+u(1, t)\,dt \tag{8}$$

where $dt$ denotes the time steplength. We then solve the conservation law using an $(s+p+1)$-step finite difference method of the form

$$a_k^{n+1}=Q(a_{k-s}^n, a_{k-s+1}^n, \cdots, a_{k+p}^n) \tag{9}$$

allowing the numerical method to continue. Before giving details of the method, it is worth making the following points:

(a) The main work in the method consists of solving the integrodifferential equation in (6).

(b) The new position of the inclusion boundaries $l(t+dt)$ has been calculated via an explicit formula. It would be possible to make this implicit but the use of terms such as $u(1, t+dt)$ would make the method computationally awkward.

(c) The finite difference method (9) is by definition explicit, and a CFL-type condition involving $dt/dx$ will no doubt have to be satisfied to ensure stability. If required, (9) could be made implicit without greatly increasing the complexity of the scheme.

(d) Equation (1) that we have solved using the finite difference method (9) is of conservation law type and therefore the development of discontinuous solutions is not out of the question. For the single conservation law

$$u_t+[f(u)]_x=0 \tag{10}$$

this will happen in general if $f''(u)<0$, and physical considerations show that this is unlikely if the inclusion is expanding. We therefore exclude this possibility for the moment.

(e) The question also arises as to the best variables for solving the integrodifferential equation (3). The function $\beta(x, t)$ appears only in a linear manner, and the absence of any derivatives of $\beta$ makes it somewhat appealing to solve for $\beta$ and determine $u(x, t)$ from this. Splines could be used to approximate $\beta$ or even merely piecewise

linear functions. There is a problem with the determination of $u$ associated with this, however. We have

$$Au_x = \int_{-l}^{x} \beta(s, t)\, ds$$

(since $A = 0$ at $x = -l$; a subsidiary result from this is that the integral of $\beta$ over the whole of the inclusion must be zero). This means that we can write $u(x, t)$ as

$$u(x, t) = \int_{\xi}^{x} \frac{1}{A(\lambda, t)} \int_{-l}^{\lambda} \beta(s, t)\, ds\, d\lambda \tag{11}$$

but the determination of $\xi$ is obvious only in the symmetrical case when $u(0, t) = 0$ and so $\xi = 0$. Furthermore, to be able to calculate the integral (11) numerically, we would in general require knowledge of $\partial u/\partial x$ at $x = \pm l$ as this is not zero at the inclusion tips. Therefore we decide to approximate $u(x, t)$ and $a(x, t)$ instead.

In view of these comments, to solve the integral equation we assume that we know $a(x, t)$ at a given time and further can approximate $a(x, t)$ as a cubic spline $T_k$ on the interval $z_k \leqq x \leqq z_{k+1}$, $(k = -N+1, \cdots, N-2)$ and a quadratic when $z_{-N} \leqq z \leqq z_{-N+1}$ or $z_{N-1} \leqq z \leqq z_N$. Also, to simplify the computations as much as possible we use a grid of constant spacing $dx = h$ and write $a_k = a(z_k)$, etc.

To approximate $u$, we define $u$ as a cubic spline when $z_{-N+1} \leqq z \leqq z_{N-1}$, and a quadratic when $z_{-N} \leqq z \leqq z_{-N+1}$ or $z_{N-1} \leqq z \leqq z_N$. Again the drop in order at the ends comes about because we do not know the derivatives of $u$ at the inclusion boundaries. This means that

$$u(x) = \begin{cases} S_k(x) & (x \in [z_k, z_{k+1}], -N+1 \leqq k < N-1), \\ L_k(x) & (x \in [z_k, z_{k+1}], k = -N \text{ or } N-1), \end{cases}$$

$$a(x) = \begin{cases} T_k(x) & (x \in [z_k, z_{k+1}], -N+1 \leqq K < N-1), \\ V_k(x) & (x \in [z_k, z_{k+1}], k = -N \text{ or } N-1) \end{cases}$$

where

$$S_k(x) = \frac{1}{6h}[M_k(z_{k+1}-x)^3 + M_{k+1}(x-z_k)^3 + (z_{k+1}-x)(6u_k - h^2M_k) + (x-z_k)(6u_{k+1} - h^2M_{k+1})],$$

$$T_k(x) = \frac{1}{6h}[N_k(z_{k+1}-x)^3 + N_{k+1}(x-z_k)^3 + (z_{k+1}-x)(6a_k - h^2N_k) + (x-z_k)(6a_{k+1} - h^2N_{k+1})],$$

$$L_{-N}(x) = (x - z_{-N+1})\left[\frac{u_{-N+1} - u_{-N}}{h} - \frac{M_{-N+1}}{2}(z_{-N} + z_{-N+1})\right] + \frac{M_{-N+1}}{2}(x^2 - z_{-N+1}^2) + u_{-N+1},$$

$$L_{N-1}(x) = (x - z_{N-1})\left[\frac{u_N - u_{N-1}}{h} - \frac{M_{N-1}}{2}(z_N + z_{N-1})\right] + \frac{M_{N-1}}{2}(x^2 - z_{N-1}^2) + u_{N-1},$$

$$V_{-N}(x)=(x-z_{-N+1})\left[\frac{a_{-N+1}-a_{-N}}{h}-\frac{N_{-N+1}}{2}(z_{-N}+z_{-N+1})\right]$$
$$+\frac{N_{-N+1}}{2}(x^2-z_{-N+1}^2)+a_{-N+1},$$
$$V_{N-1}(x)=(x-z_{N-1})\left[\frac{a_N-a_{N-1}}{h}-\frac{N_{N-1}}{2}(z_N+z_{N-1})\right]+\frac{N_{N-1}}{2}(x^2-z_{N-1}^2)+a_{N-1},$$

and $u_k=u(z_k)$, $a_k=a(z_k)$ with standard spline equations

$$5M_{-N+1}+M_{-N+2}=\frac{6}{h^2}[u_{-N+2}-2u_{-N+1}+u_{-N}],$$
$$M_{N-2}+5M_{N-1}=\frac{6}{h^2}[u_{N-2}-2u_{N-1}+u_N], \tag{12}$$
$$M_{k-1}+4M_k+M_{k+1}=\frac{6}{h^2}[u_{k-1}-2u_k+u_{k+1}] \qquad (k=-N+2,\cdots,N-2),$$
$$5N_{-N+1}+N_{-N+2}=\frac{6}{h^2}[a_{-N+2}-2a_{-N+1}+a_{-N}],$$
$$N_{N-2}+5N_{N-1}=\frac{6}{h^2}[a_{N-2}-2a_{N-1}+a_N], \tag{13}$$
$$N_{k-1}+4N_k+N_{k+1}=\frac{6}{h^2}[a_{k-1}-2a_k+a_{k+1}] \qquad (k=-N+2,\cdots,N-2).$$

Having given the details of the splines that we are using, we now note that actually a more convenient way of expressing them is by setting

$$u(x)=S_k(x), \qquad a(x)=T_k(x)$$

for $x\in[z_k, z_{k+1}]$ $(k=-N,\cdots,N-1)$ and defining $M_{-N}$ and $M_N$ so that $M_{-N}=M_{-N+1}$ and $M_{N-1}=M_N$, with similar conventions for $N_{-N}$ and $N_N$. It is easily shown that this gives the same formulae for the splines as before, and in fact this corresponds to specifying that the curvature at the endpoints of the inclusion is the same as the curvature at the penultimate points. Clearly with a large enough grid this should cause no problems. If we assume now that the values of the $2N+1$ constants $u_{-N},\cdots,u_N$ are "known," then we have $2+1+2(N-2)+2=2N+1$ equations for the $2N+1$ parameters $M_{-N},\cdots,M_N$. The integral equation must therefore provide us with $2N+1$ equations for the values $u_{-N},\cdots,u_N$. This is ensured by collocation carried out in the following manner. Collocating at the points $z_L$ $(L=-N,\cdots,N)$ we let

$$I_{k,L}=\int_{z_k}^{z_{k+1}}\frac{B(p,t)-B(z_L,t)}{|p-z_L|}\,dp$$

and approximate the integral equation in (6) by

$$\sum_{k=-N}^{N-1} I_{k,L}+B(z_L,t)\left[C+\log\left(\frac{1-z_L^2}{a(z_L)}\right)\right]+\frac{4\pi\lambda}{3}[lz_L-u(z_L)]=0 \tag{14}$$
$$(L=-N,\cdots,N).$$

The integrals $I_{k,L}$ are in principle easy but in practice awkward to calculate (a symbolic algebra package such as MAPLE is the easiest way to perform them) and details are

given in Appendix (i), but having calculated them we can now set up the required linear equations. First of all, we let $\mathbf{q}$ represent the $(4N+2)\times 1$ vector

$$\mathbf{q}=(u_{-N}, M_{-N}, u_{-N+1}, M_{-N+1}, \cdots, u_{N-1}, M_{N-1}, u_N, M_N)^T.$$

We wish to write (12) and (14) as

$$E\mathbf{q}=\mathbf{b}$$

and we note immediately that there is no point in trying to achieve banding of the matrix $E$ as most of the entries will be nonzero. To be more specific, we write

$$E=\left[\frac{E_1}{E_2}\right], \qquad \mathbf{b}=\left[\frac{\mathbf{b}_1}{\mathbf{b}_2}\right]$$

where $E_1$ covers (12) and $E_2$ covers (14), and a similar convention is adopted for the components $\mathbf{b}_1$ and $\mathbf{b}_2$ of the right-hand side $\mathbf{b}$. The $(2N+1)\times(4N+2)$ matrix $E_1$ is banded with a bandwidth of six while the $(2N+1)\times 1$ vector $\mathbf{b}_1=0$, however, the structure of the $(2N+1)\times(4N+2)$ matrix $E_2$ is more complicated. For simplicity it is convenient to split $E_2$ into three parts so that

$$E_2=E_2^{(1)}+E_2^{(2)}+E_2^{(3)}.$$

Taking these one by one, $E_2^{(1)}$ is defined as the part of the matrix that is NOT due to the integral terms $I_{k,L}$. Writing (14) in order from $L=-N$ to $N$, we find that the structure of this part of the matrix is given by

$$\begin{aligned}
E^{(1)}_{2(2N+2,1)}&=-6K_{-N}H_{-N}-4\pi\lambda/3,\\
E^{(1)}_{2(2N+2,2)}&=H_{-N}[-2h^2K_{-N}+a_{-N}],\\
E^{(1)}_{2(2N+2,3)}&=6K_{-N}H_{-N},\\
E^{(1)}_{2(2N+2,4)}&=-h^2K_{-N}H_{-N},\\
E^{(1)}_{2(K,2K-4N-3)}&=-6K_{K-3N-2}-4\pi\lambda/3,\\
E^{(1)}_{2(K,2K-4N-2)}&=H_{K-3N-2}[-2h^2K_{K-3N-2}+a_{K-3N-2}],\\
E^{(1)}_{2(K,2K-4N-1)}&=6K_{K-3N-2}H_{K-3N-2},\\
E^{(1)}_{2(K,2K-4N)}&=-h^2K_{K-3N-2}H_{K-3N-2},\\
E^{(1)}_{2(4N+2,4N-1)}&=-6K_NH_N,\\
E^{(1)}_{2(4N+2,4N)}&=h^2K_NH_N,\\
E^{(1)}_{2(4N+2,4N+1)}&=6K_NH_N-4\pi\lambda/3,\\
E^{(1)}_{2(4N+2,4N+2)}&=H_N[2h^2K_N+a_N]
\end{aligned}$$

$$(K=2N+3,\cdots,4N+1),$$

where

$$K_L=\frac{1}{36h^2}[-2h^2N_L-6a_L+6a_{L+1}-h^2N_{L+1}],$$

$$K_N=\frac{1}{36h^2}[2h^2N_N-6a_{N-1}+6a_N+h^2N_{N-1}]$$

and

$$H_L=C+\log\left(\frac{1-z_L^2}{a(z_L)}\right).$$

At the endpoints, we evaluate this logarithmic term using a linear approximation for $a$, so that, for example,

$$H_N = C + \log\left(\frac{2h}{a_{N-1}}\right).$$

Now we consider the contributions from the $I_{k,L}$ terms. Using Appendix (i), each term in the integral has a "$K$" component involving $M_{k+1}$, $M_k$, $u_k$, and $u_{k+1}$, and also an "$L$" component involving $M_L$, $M_{L+1}$, $M_{L-1}$, $u_L$, $u_{L+1}$, and $u_{L-1}$. We define $E_2^{(2)}$ to be the part of the $(2N+1)\times(4N+2)$ submatrix $E_2$ that involves the "$K$" component, and $E_2^{(3)}$ the part that involves the "$L$" component. After some further computations, we find that $E_2^{(2)}$ is given for $K = 2N+2, \cdots, 4N+2$ by

$$\begin{aligned} E^{(2)}_{2(K,2I+2)} &= \nu\Lambda^{(1)}_{I-N,K-3N-2}, \\ E^{(2)}_{2(K,2I+1)} &= \nu\Lambda^{(3)}_{I-N,K-3N-2}, \end{aligned} \qquad I = 0, \cdots, 2N-1,$$

$$\nu = \begin{cases} -1 & \text{if } K - I \geqq 2N+3, \\ 1 & \text{otherwise,} \end{cases}$$

$$\begin{aligned} E^{(2)}_{2(K,2I+2)} &= E^{(2)}_{2(K,2I+2)} + \nu\Lambda^{(2)}_{I-N-1,K-3N-2}, \\ E^{(2)}_{2(K,2I+1)} &= E^{(2)}_{2(K,2I+1)} + \nu\Lambda^{(4)}_{I-N-1,K-3N-2}, \end{aligned} \qquad I = 1, \cdots, 2N,$$

$$\nu = \begin{cases} -1 & \text{if } K - I \geqq 2N+2, \\ 1 & \text{otherwise} \end{cases}$$

(see Appendix (i) for the definition of the $\Lambda$s) and it only remains to determine $E_2^{(3)}$. Using the fact that some of the logarithmic sums telescope, we find eventually that we may write the submatrix $E_2^{(3)}$ as

$$\begin{aligned} E^{(3)}_{2(2N+2,1)} &= \bar{\Lambda}^{(7)}_{-N} \log(2N), \\ E^{(3)}_{2(2N+2,2)} &= \bar{\Lambda}^{(5)}_{-N} \log(2N), \\ E^{(3)}_{2(2N+2,3)} &= \bar{\Lambda}^{(8)}_{-N} \log(2N), \\ E^{(3)}_{2(2N+2,4)} &= \bar{\Lambda}^{(6)}_{-N} \log(2N), \end{aligned}$$

$$\begin{aligned} E^{(3)}_{2(K,2K-4N-3)} &= \bar{\Lambda}^{(7)}_{K-3N-2} \log((K-2N-2)(4N+2-K)) \\ E^{(3)}_{2(K,2K-4N-2)} &= \bar{\Lambda}^{(5)}_{K-3N-2} \log((K-2N-2)(4N+2-K)) \\ E^{(3)}_{2(K,2K-4N-1)} &= \bar{\Lambda}^{(8)}_{K-3N-2} \log((K-2N-2)(4N+2-K)) \\ E^{(31)}_{2(K,2K-4N)} &= \bar{\Lambda}^{(6)}_{K-3N-2} \log((K-2N-2)(4N+2-K)) \end{aligned} \qquad (K = 2N+3, \cdots, 4N+1),$$

$$\begin{aligned} E^{(3)}_{2(4N+2,4N-1)} &= \bar{\Lambda}^{(9)}_{N} \log(2N), \\ E^{(3)}_{2(4N+2,4N)} &= \bar{\Lambda}^{(10)}_{N} \log(2N), \\ E^{(3)}_{2(4N+2,4N+1)} &= \bar{\Lambda}^{(7)}_{N} \log(2N), \\ E^{(3)}_{2(4N+2,4N+2)} &= \bar{\Lambda}^{(5)}_{N} \log(2N) \end{aligned}$$

where the bar denotes that $\bar{\Lambda}^{(5)}_{i,-N}$ is the same as $\Lambda^{(5)}_{i,-N}$, but with the log term set to unity. It now remains only to determine the right-hand side vector $\mathbf{b}_2$. This is composed only of the nonhomogeneous term of (14), so that

$$\mathbf{b}_2 = \frac{4l(t)\pi\lambda}{3}(-z_{-N}, -z_{-N+1}, \cdots, -z_{N-1}, -z_N)^T$$

and the simultaneous linear equation formulation of (12) and (14) is complete. The final structure of the matrix $E$ is such that the bottom half of the matrix is full and the top half of the matrix is banded of bandwidth six. This confirms our earlier statement that there is no point in trying to use sparse solvers, and accordingly the NAG routine F04ATF was used for the solution of the equations, while the much quicker F04FAF was used to solve the equations for the spline coefficients of $a$.

For the timestepping procedure to solve the conservation law, the Lax-Friedrichs method was used. The equation

$$(l^3a)_t+[l^2ua-z\dot{l}l^2a]_z=0$$

was written

$$w_t+f(w)_x=0 \qquad (w=l^3a)$$

and discretized as

$$w_i^{n+1}=\frac{1}{2}[w_{i+1}^n+w_{i-1}^n]-\left(\frac{dt}{2dx}\right)[f_{i+1}^n-f_{i-1}^n].$$

The relevant Courant number may be estimated by writing the conservation law as

$$w_t+\left(w\left[\frac{u}{l}-\frac{z\dot{l}}{l}\right]\right)_z=0$$

so that

$$w_t+\left(\frac{u}{l}-\frac{z\dot{l}}{l}\right)w_z+w\left(\frac{u_z}{l}-\frac{\dot{l}}{l}\right)=0,$$

and assuming that $u$ is "known" we find that the Courant number $\mathscr{C}$, that must be less than unity for stability, is given by

$$\mathscr{C}=\max_{z\in[-1,1]}\left[\left(\frac{u-z\dot{l}}{l}\right)\frac{dt}{dx}\right].$$

As usual in the solution of such equations, it is desirable to keep the Courant number as close to unity as possible for an accurate solution, but it is interesting to note that in the case of the exact solution (see Part I [7]) the Courant number is always identically zero. This of course is a consequence of the fact that the exact solution is a true similarity solution, so that with a suitable choice of new independent coordinates the evolution is only in one variable.

For the numerical results described below, the coding was carried out in FORTRAN 77 and a DIGITAL VAX 8700 was used for the calculations.

**4. The asymmetrical case.** Before giving a selection of numerical results that were calculated using the method described above, it is worth making a brief comment on the asymmetrical case. The relevant equation is (2) and once again it is possible to simplify this and fix the mesh by setting

$$x=\tfrac{1}{2}[(l_2-l_1)+(l_1+l_2)z],$$

$$A=\left(\frac{l_1+l_2}{2}\right)^2 a(z,t),$$

$$s=\tfrac{1}{2}[(l_2-l_1)+(l_1+l_2)p] \quad \text{in the integral,}$$

and

$$B(z,t)=\frac{3}{8\pi\lambda}(Au_x)_x.$$

Equation (2) is then transformed to

$$\int_{-1}^{1} \frac{B(p,t)-B(z,t)}{|p-z|}\,dp + B(z,t)\left[C+\log\left(\frac{1-z^2}{a}\right)\right] + \frac{4\pi\lambda}{3}\left(\frac{1}{2}[(l_2-l_1)+(l_1+l_2)z]-u\right)=0 \qquad \left(C=-1-\log\left(\frac{\varepsilon^2}{4\pi}\right)\right)$$

and the corresponding boundary conditions are

$$A=0 \quad \text{at } z=\pm 1,$$

$$u(-1,t)=-\dot{l}_1(t), \qquad u(1,t)=\dot{l}_2(t).$$

The conservation law becomes

$$[l^{*3}a]_t+\left[l^{*2}au-l^{*2}a\frac{\dot{l}_2-\dot{l}_1+z(\dot{l}_1+\dot{l}_2)}{2}\right]_z=0$$

where

$$l^*=\frac{l_1+l_2}{2}$$

and we may define the Courant number $\mathscr{C}$ in the obvious way by

$$\mathscr{C}=\max_{z\in[-1,1]}\left[\left(\frac{2u-z(\dot{l}_1+\dot{l}_2)-\dot{l}_2+\dot{l}_1}{2l^*}\right)\frac{dt}{dx}\right].$$

The changes required to be able to treat the asymmetrical problem are therefore minimal and amount to no more than a change in the right-hand sides of the linear equations and the need to keep track of two lengths and their derivatives in the timestepping procedure.

**5. Numerical results.** The first test of the numerical scheme consisted of reproducing the known exact solution for the case where the initial shape of the inclusion was spheroidal. Figure 1(a) shows the cross-sectional area $A(x, t)$ at time $t=4$, for the case $\varepsilon=0.1$. Here and henceforth $\lambda$ will have the value unity. Figure 1(b) shows the logarithm of the inclusion halflength $l(t)$ as a function of time. Here calculations were made

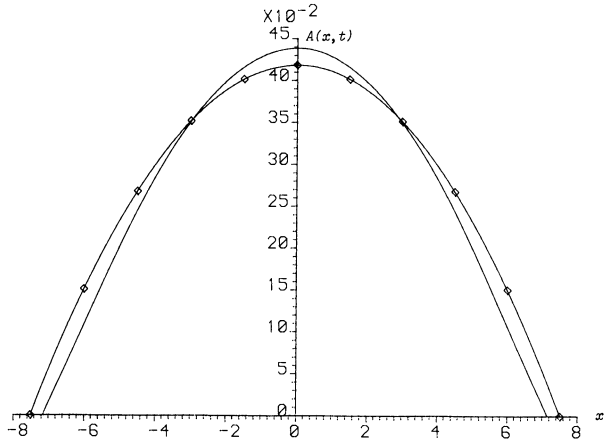


FIG. 1(a). *Comparison between exact (line and symbol) and computed (solid line) cross-sectional areas at time $t=4$ for an initially spheroidal inclusion with $\varepsilon=0.1$, $\lambda=1$.*

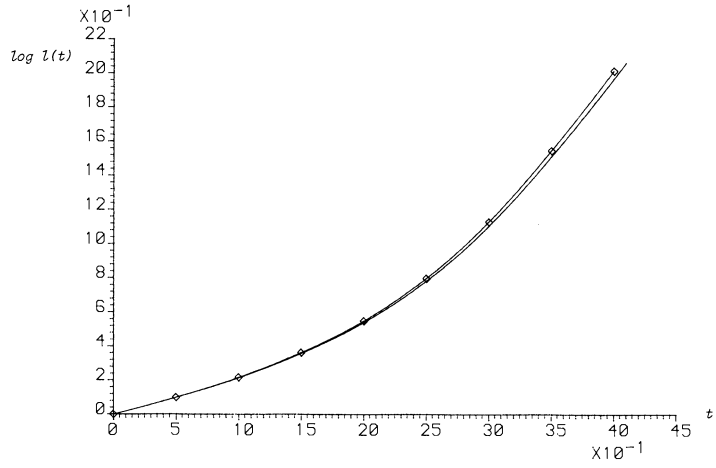


FIG. 1(b). *Comparison between exact (line and symbol) and computed (solid line) inclusion half-lengths at time* $t=4$ *for an initially spheroidal inclusion with* $\varepsilon=0.1$, $\lambda=1$.

with 50 meshpoints in each half of the inclusion and a timestep of 0.05. The exact solution is denoted by the line and symbol, while the computed results are shown as a full line. At time $t=4$ (after 80 timesteps) the ratio of the inclusion volume to the original volume has fallen by four percent. A result of this is that mass is being lost from the ends and gained at the center. Agreement is clearly good, indicating that the numerical method is working well.

Next we considered a case where the initial shape of the inclusion had a neck at $x=0$, but was symmetrically placed about the origin. The characteristic "shouldered" shape was given by

$$A(x,0)=(1-x^2)\left[\left(\frac{119}{8}-\frac{35\pi}{4}\right)x^4+\left(\frac{35\pi}{4}-\frac{131}{8}\right)x^2+2\right]$$

and the slenderness parameter $\varepsilon$ was chosen to be 0.1. Fifty meshpoints were used in each half of the inclusion and the Courant number was fixed at 0.5. The results are shown in Figs. 2(a) (times $t=0$, 2, and 4) and 2(b). It should be noted that initially

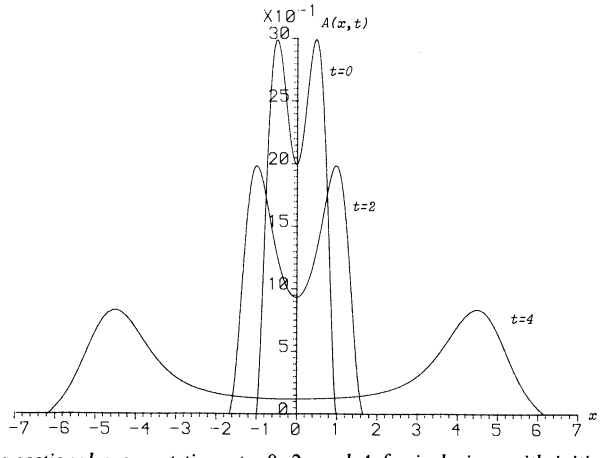


FIG. 2(a). *Cross-sectional areas at times* $t=0$, 2, *and* 4 *for inclusions with initial "shouldered" profile* ($\varepsilon=0.1$, $\lambda=1$).

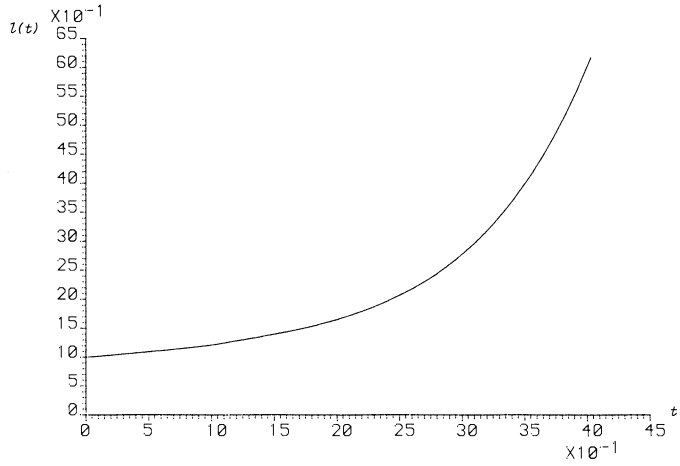


FIG. 2(b). *Inclusion half-length for inclusion with initial "shouldered" profile* ($\varepsilon = 0.1$, $\lambda = 1$).

the ratio of the cross-sectional areas at the peak and trough is 1.5, while later this ratio increases; for example at $t = 4$, where two percent of the volume has been lost, it has risen to approximately seven. This leads to a more rapid thinning at the center of the inclusion so that at later times the shape resembles a "dumbbell." This dumbbell shape is maintained for large times in the form of the limiting similarity solution described in Part I [7]. This result is reminiscent of glass-drawing (see [3]).

As an example of an asymmetrical problem, we took the initial cross-sectional area as

$$A(x, 0) = \pi(1 - x^2)(x + 1), \tag{15}$$

choosing $\varepsilon = 0.1$ and utilizing 75 meshpoints in each half of the inclusion with a Courant number of 0.5. The endpoints were chosen as $x = \pm 1$ so that the inclusion was symmetrically placed about the origin. Results for the cross-sectional area $A(x, t)$ at various times and the inclusion lengths $l_1(t)$ and $l_2(t)$ are shown in Figs. 3(a) (times $t = 0$, 1.5, and 3.0) and 3(b). At time $t = 3$ the loss in volume is 12 percent. The bulk

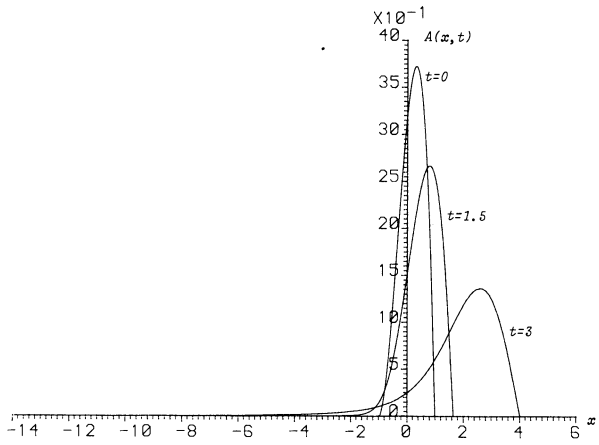


FIG. 3(a). *Cross-sectional areas at times* $t = 0$, 1.5, *and* 3 *for inclusion with initial asymmetrical profile* ($\varepsilon = 0.1$, $\lambda = 1$).

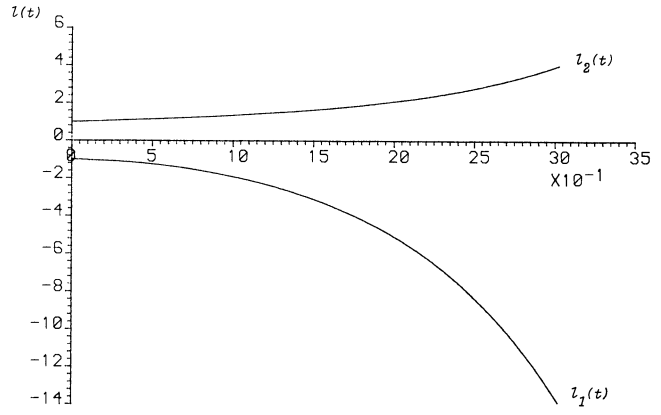


FIG. 3(b). *Inclusion half-length for inclusion with initial asymmetrical profile* ($\varepsilon = 0.1$, $\lambda = 1$).

of the inclusion moves off to the right, but the velocity of the left-hand endpoint is much greater than that of the right.

To verify some of the results that have been obtained at the end of Part I, the above asymmetrical example was run first with a much smaller value of $\varepsilon$ ($1.0 \times 10^{-8}$) and with the inclusion symmetrically placed, and again for the same value of $\varepsilon$ but with the ends at $x = 0$ and $x = 2$. In both cases, 100 meshpoints were used for each half of the inclusion and the Courant number was 0.9. The results are shown in Figs. 4(a) and 4(b), and 5(a) and 5(b), respectively. In the former case, the inclusion does not move substantially until time $t = 2$, when it begins to move rapidly to the left and tends to the similarity solution. This is the expected result. At $t = 2$ it has lost six percent of its volume. For small times, the right-hand end moves slightly to the right before changing direction and progressing to the left. This behavior occurs for sufficiently small values of $\varepsilon$ for the same initial shape when the inclusion begins symmetrically placed. It is also worth noting that although the values of $l_1(t)$ increase rapidly after time $t = 2$, for much of the left-hand end of the inclusion the cross-sectional area is negligible. In the latter case the behavior is quite different as the inclusion is initially placed with all of its volume to the right of the origin. Now the inclusion

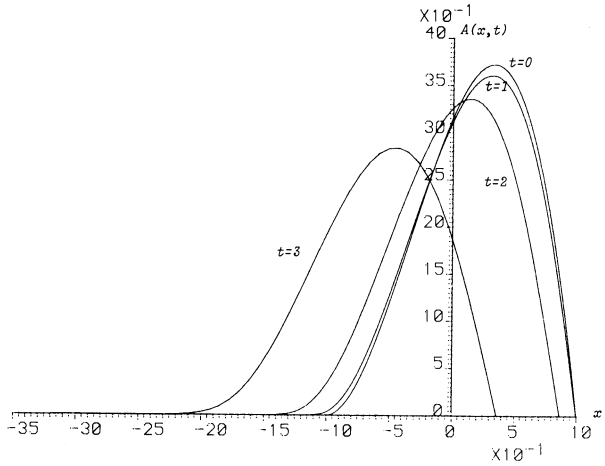


FIG. 4(a). *Cross-sectional areas at times* $t = 0$, 1, 2, *and* 3 *for inclusion with initial asymmetrical profile with endpoints symmetrically placed about the origin* ($\varepsilon = 1 \times 10^{-8}$, $\lambda = 1$).

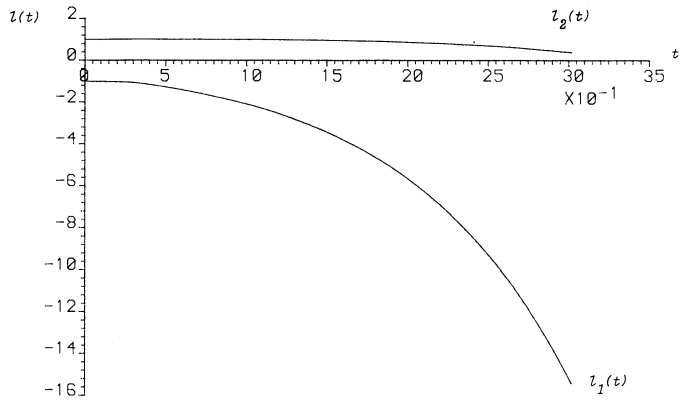


FIG. 4(b). *Inclusion half-length for inclusion with initial asymmetrical profile with endpoints symmetrically placed about the origin* ($\varepsilon = 1 \times 10^{-8}$, $\lambda = 1$).

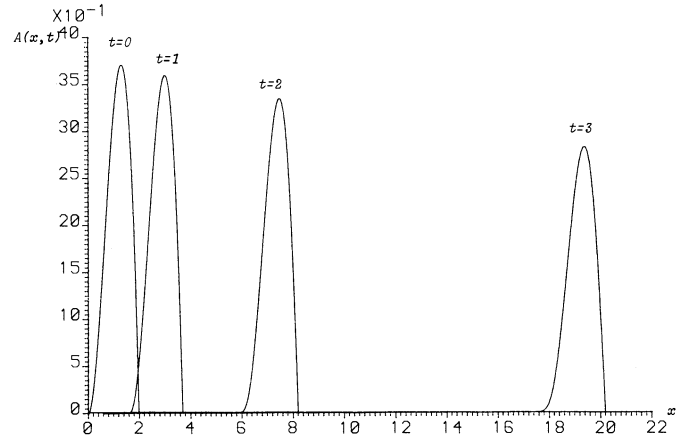


FIG. 5(a). *Cross-sectional areas at times* $t = 0$, 1, 2, *and* 3 *for inclusion with initial asymmetrical profile and endpoints asymmetrically placed about the origin* ($\varepsilon = 1 \times 10^{-8}$, $\lambda = 1$).

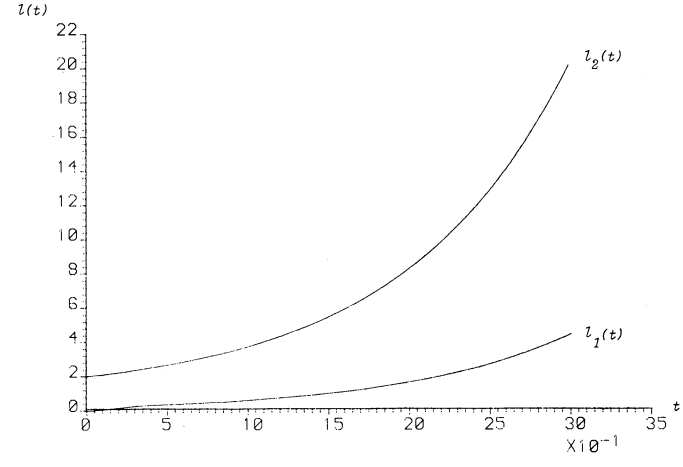


FIG. 5(b). *Inclusion half-length for inclusion with initial asymmetrical profile and endpoints asymmetrically placed about the origin* ($\varepsilon = 1 \times 10^{-8}$, $\lambda = 1$).

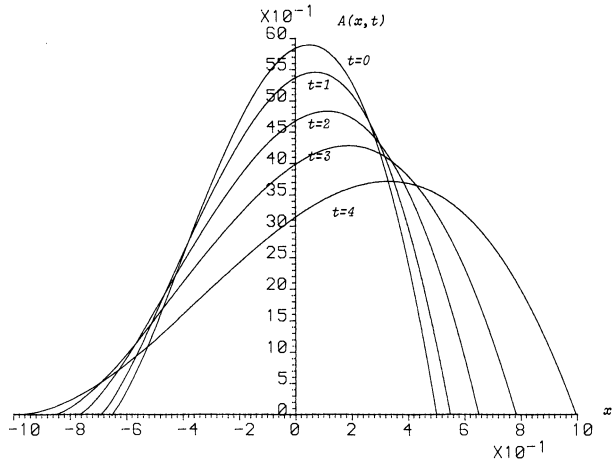


FIG. 6(a). *Cross-sectional areas at times* $t = 0, 1, 2, 3,$ *and* 4 *for inclusion with initial asymmetrical profile, flow reversed* ($\varepsilon = 0.1$, $\lambda = 1$).

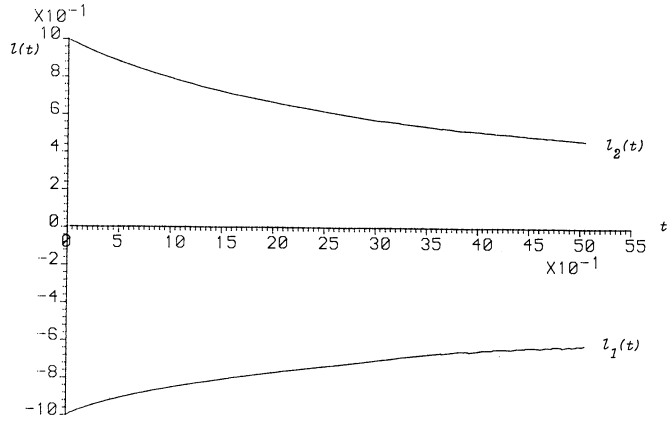


FIG. 6(b). *Inclusion half-length for inclusion with initial asymmetrical profile, flow reversed* ($\varepsilon = 0.1$, $\lambda = 1$).

moves off to the right immediately with much greater speed and takes the form of the similarity solution, again as predicted by the theory. By time $t = 2$ it has lost five percent of its volume. Again we note that to the left of the inclusion at later times there is a considerable "tail" with negligible cross-sectional area.

The final example considered corresponded to a reversed outer flow, so that in (2) the leftmost term $x$ on the left-hand side is simply replaced by $-x$. We again used the initial profile (15) with $\varepsilon = 0.1$ and performed calculations with 100 meshpoints in each half of the inclusion and a Courant number of 0.9. The results are shown in Figs. 6(a) and 6(b) and indicate that the inclusion is being compressed while losing its asymmetry. Because the total length of the inclusion in this problem decreases, there is little loss in volume, barely one percent having been lost at time $t = 4$.

**6. Conclusions and discussion.** A numerical method has been proposed for the solution of an integrodifferential equation coupled with a conservation law. The method appears to agree well with known theory and allows accurate computations to be made of the motion of a viscous inclusion. Conclusions from limiting cases of the theory have also been confirmed and the numerical method has proved to be robust.

**Appendix (i).** To determine the entries in the matrix $E$, which is required to solve the integrodifferential equation, there are a number of basic cases we must consider for the integral

$$I_{k,L}=\int_{z_k}^{z_{k+1}}\frac{B(p,t)-B(z_L,t)}{|p-z_L|}\,dp.$$

For $-N\leqq k\leqq N-1$ these are (i) $L<k$, (ii) $L>k+1$, (iii) $L=k$, and (iv) $L=k+1$. For convenience we write (taking case (i) first)

$$\begin{aligned}a(x)=T_k(x)=\frac{1}{6h}\,&(N_k(z_{k+1}-z_L+z_L-x)^3+N_{k+1}(x-z_L+z_L-z_k)^3\\&+(z_{k+1}-z_L+z_L-x)(6a_k-h^2N_k)\\&+(x-z_L+z_L-z_k)(6a_{k+1}-h^2N_{k+1})),\end{aligned}$$

$$\begin{aligned}u(x)=S_k(x)=\frac{1}{6h}\,&(M_k(z_{k+1}-z_L+z_L-x)^3+M_{k+1}(x-z_L+z_L-z_k)^3\\&+(z_{k+1}-z_L+z_L-x)(6u_k-h^2M_k)\\&+(x-z_L+z_L-z_k)(6u_{k+1}-h^2M_{k+1}))\end{aligned}$$

for $x\in[z_k,z_{k+1}]$ and we find that

$$\begin{aligned}a&=A_k^a(x-z_L)^3+B_{kL}^a(x-z_L)^2+C_{kL}^a(x-z_L)+D_{kL}^a,\\u&=A_k^u(x-z_L)^3+B_{kL}^u(x-z_L)^2+C_{kL}^u(x-z_L)+D_{kL}^u\end{aligned}$$

where

$$A_k^a=\frac{1}{6h}(N_{k+1}-N_k),\qquad B_{kL}^a=\frac{1}{2h}[N_k(z_{k+1}-z_L)+N_{k+1}(z_L-z_k)],$$

$$C_{kL}^a=\frac{1}{6h}[3N_{k+1}(z_L-z_k)^2-3N_k(z_{k+1}-z_L)^2+6(a_{k+1}-a_k)+h^2(N_k-N_{k+1})],$$

$$\begin{aligned}D_{kL}^a=\frac{1}{6h}\,&[N_k(z_{k+1}-z_L)^3+N_{k+1}(z_L-z_k)^3\\&+(z_{k+1}-z_L)(6a_k-h^2N_k)+(z_L-z_k)(6a_{k+1}-h^2N_{k+1})]\end{aligned}$$

and the $A_k^u$'s, $B_{kL}^u$'s etc. are defined in the same way but with $M$ replacing $N$ and $u$ replacing $a$. We may now compute

$$B=(au_x)_x=a_xu_x+au_{xx}$$

and we find that for $x\in[z_k,z_{k+1}]$

$$B(x)=E_k(x-z_L)^4+F_{kL}(x-z_L)^3+G_{kL}(x-z_L)^2+H_{kL}(x-z_L)+J_{kL}$$

where

$$\begin{aligned}E_k&=15A_k^aA_k^u,\qquad F_{kL}=12A_k^uB_{kL}^a+8A_k^aB_{kL}^u,\\G_{kL}&=6B_{kL}^uB_{kL}^a+9C_{kL}^aA_k^u+3C_{kL}^uA_k^a,\\H_{kL}&=4B_{kL}^uC_{kL}^a+6A_k^uD_{kL}^a+2B_{kL}^aC_{kL}^u,\\J_{kL}&=C_{kL}^uC_{kL}^a+2D_{kL}^aB_{kL}^u.\end{aligned}$$

Now for $L<k$, we have

$$I_{kL}=\int_{z_k}^{z_{k+1}}\frac{B(x)-B(z_L)}{x-z_L}\,dx$$

and so from a simple integration, we find that

$$I_{kL}=\frac{E_k}{4}\phi_4+\frac{F_{kL}}{3}\phi_3+\frac{G_{kL}}{2}\phi_2+hH_{kL}+[J_{kL}-B(z_L)]\log\left(\frac{z_{k+1}-z_L}{z_k-z_L}\right)$$
$$=Q_{kL}\quad\text{say}$$

where

$$\phi_P=(z_{k+1}-z_L)^P-(z_k-z_L)^P.$$

Also for $L>k+1$ we find that

$$I_{kL}=-Q_{kL}$$

as the modulus term simply contributes a factor of $-1$. Naturally in the cases $L=k$, $k+1$ we must check that there is no singularity. For $L=k$, we have

$$B(z_L)=J_{LL}=J_{kL}|_{k=L}$$

so there are no problems. For $L=k+1$ we have

$$B(z_L)=J_{k+1,L}$$

and so we must show that

$$J_{L,L}=J_{L-1,L}.$$

This however is easily checked from the definitions. The only remaining singular case to check is when $k=N+1$, $L=N$ as we use a different form for $B$ here. We have

$$B(z_L)=J_{N-1,N}=J_{kL}|_{L=N,k=N-1}$$

and so the singularity is duly removed here also. (We have ensured the continuity of $u_{xx}$ by employing cubic splines for $u$.) We therefore find that

$$I_{kL}=\begin{cases}Q_{kL}, & L=-N,-N+1,\cdots,k-1,\\ -Q_{kL}, & L=k+2,\cdots,N-1,N,\\ Q^*_{kL}, & L=k,\\ -Q^*_{kL}, & L=k+1\end{cases}$$

where $Q^*_{kL}=(Q_{kL}$ with the log term omitted). Noting that from the definitions we have

$$B(z_L)=\left(\frac{1}{6h}\right)^2[-2h^2N_L-h^2N_{L+1}+6(a_{L+1}-a_L)]$$
$$\cdot[-2h^2M_L-h^2M_{L+1}+6(u_{L+1}-u_L)]+a_LM_L\qquad(L<N),$$
$$B(z_N)=\left(\frac{1}{6h}\right)^2[2h^2N_N+h^2N_{N-1}+6(-a_{N+1})]$$
$$\cdot[2h^2M_N+h^2M_{N-1}+6(u_N-u_{N-1})]\qquad(L=N).$$

It is a simple but lengthy job to show that

$$Q_{kL}=\Lambda^{(1)}_{kL}M_k+\Lambda^{(2)}_{kL}M_{k+1}+\Lambda^{(3)}_{kL}u_k+\Lambda^{(4)}_{kL}u_{k+1}+\Lambda^{(5)}_{kL}M_L$$
$$+\Lambda^{(6)}_{kL}M_{L+1}+\Lambda^{(7)}_{kL}u_L+\Lambda^{(8)}_{kL}u_{L+1}+\Lambda^{(9)}_{kL}u_{L-1}+\Lambda^{(10)}_{kL}M_{L-1}$$

where

$$\left(r = L-k,\ \Upsilon = \log\left(\frac{r-1}{r}\right)\right),$$

$$\Lambda_{kL}^{(1)} = h^2 N_k\left[-\frac{53}{144}+\frac{r}{72}(106-105r+30r^2)+\left[\frac{1}{9}+\frac{r}{12}(r-2)(6-10r-5r^2)\right]\Upsilon\right]$$
$$+h^2 N_{k+1}\left[-\frac{25}{144}-\frac{r}{72}(-20-33r+30r^2)\right.$$
$$\left.+\left[\frac{1}{18}-\frac{r}{12}(r-1)(-4-3r+5r^2)\right]\Upsilon\right]+\alpha_k\left[-\frac{9}{4}+\frac{3r}{2}+\left(\frac{4}{3}-3r+\frac{3r^2}{2}\right)\Upsilon\right]$$
$$+a_{k+1}\left[\frac{5}{4}-\frac{3r}{2}+\left(-\frac{1}{3}+2r-\frac{3r^2}{2}\right)\Upsilon\right],$$

$$\Lambda_{kL}^{(2)} = h^2 N_k\left[-\frac{7}{48}-\frac{r}{72}(4-57r+30r^2)\right.$$
$$\left.+\left[\frac{1}{18}-\frac{r}{12}(r-1)(-2-7r+5r^2)\right]\Upsilon\right]+h^2 N_{k+1}\left[-\frac{1}{16}+\frac{r}{72}(-14+15r+30r^2)\right.$$
$$\left.+\left[\frac{1}{36}-\frac{r^2}{12}(-4+5r^2)\right]\Upsilon\right]+a_k\left[\frac{1}{4}-\frac{3r}{2}+\left(\frac{1}{6}+r-\frac{3r}{2}\right)\Upsilon\right]$$
$$+a_{k+1}\left[\frac{3}{4}+\frac{3r}{2}+\left(-\frac{1}{6}+\frac{3r^2}{2}\right)\Upsilon\right],$$

$$\Lambda_{kL}^{(3)} = N_k\left(-\frac{3}{4}+\frac{r}{2}\right)+N_{k+1}\left(-\frac{1}{4}-\frac{r}{2}\right)+\Upsilon\left[\frac{a_k-a_{k+1}}{h^2}+N_k\left(\frac{1}{3}-r+\frac{r^2}{2}\right)+N_{k+1}\left(\frac{1}{6}-\frac{r^2}{2}\right)\right],$$

$$\Lambda_{kL}^{(4)} = -\Lambda_{kL}^{(3)},$$

$$\Lambda_{kL}^{(5)} = \begin{cases} -\Upsilon\left[\dfrac{h^2}{9}N_L+\dfrac{h^2}{18}N_{L+1}-\dfrac{1}{3}a_{L+1}+\dfrac{4}{3}a_L\right] & (L<N), \\ -\Upsilon\left[\dfrac{h^2}{9}N_N-\dfrac{1}{3}a_{N-1}+\dfrac{h^2}{18}N_{N-1}\right] & (L=N), \end{cases}$$

$$\Lambda_{kL}^{(6)} = \begin{cases} -\Upsilon\left[\dfrac{h^2}{18}N_L+\dfrac{h^2}{36}N_{L+1}-\dfrac{1}{6}a_{L+1}+\dfrac{1}{6}a_L\right] & (L<N), \\ 0 & (L=N), \end{cases}$$

$$\Lambda_{kL}^{(7)} = \begin{cases} -\Upsilon\left[\dfrac{1}{3}N_L+\dfrac{1}{6}N_{L+1}-\dfrac{1}{h^2}(a_{L+1}-a_L)\right] & (L<N), \\ -\Upsilon\left[\dfrac{1}{3}N_N-\dfrac{1}{h^2}a_{N-1}+\dfrac{1}{6}N_{N-1}\right] & (L=N), \end{cases}$$

$$\Lambda_{kL}^{(8)} = \begin{cases} -\Lambda_{kL}^{(7)} & (L<N), \\ 0 & (L=N), \end{cases}$$

$$\Lambda_{kL}^{(9)} = \begin{cases} 0 & (L<N), \\ -\Lambda_{kL}^{(7)} & (L=N), \end{cases}$$

$$\Lambda_{kL}^{(10)} = \begin{cases} 0 & (L<N), \\ -\Upsilon\left[\dfrac{h^2}{18}N_N-\dfrac{1}{6}a_{N-1}+\dfrac{h^2}{36}N_{N-1}\right] & (L=N). \end{cases}$$

## REFERENCES

[1] C. T. H. BAKER, *The Numerical Treatment of Integral Equations*, Clarendon Press, Oxford, 1978.

[2] L. M. DELVES AND J. WALSH, *Numerical Solution of Integral Equations*, Clarendon Press, Oxford, 1974.

[3] J. DEWYNNE, J. R. OCKENDON, AND P. WILMOTT, *On a mathematical model for glass-fibre tapering*, SIAM J. Appl. Math., 49 (1989), pp. 983-991.

[4] A. D. FITT, *Numerical solutions of a certain class of non-linear singular integro-differential equations*, Cranfield Institute of Technology, Mathematics and Ballistics Group Report No. MB 7/86, Bedford, 1986.

[5] ———, *A note on the numerical solution of a finite-range singular integro-differential equation*, Cranfield Institute of Technology, Mathematics and Ballistics Group Report No. MB 2/87, Bedford, 1987.

[6] D. A. SPENCE AND P. SHARP, *Self-similar solutions for elastohydrodynamic cavity flow*, Proc. Roy. Soc. London Ser. A, 400 (1985), pp. 289-313.

[7] P. WILMOTT, *The stretching of a slender, axisymmetric, viscous inclusion—Part* I: *asymptotic analysis*, SIAM J. Appl. Math., this issue, pp. 1608-1616.